In-Plane Behavior of the *Dhajji-Dewari* Structural System (Wooden Braced Frame with Masonry Infill)

Qaisar Ali,[a] Tom Schacher,[b] Mohammad Ashraf,[a] Bashir Alam,[a] Akhtar Naeem,[a] Naveed Ahmad,[a] and Muhammad Umar[a]

This paper presents experimental and numerical investigations conducted on typical *dhajji* buildings found in the northern mountainous areas of Kashmir and surrounding regions to evaluate their in-plane lateral load response. The experimental work included an in-plane quasistatic cyclic test on three full-scale walls as well as monotonic tension and bend tests on main connections. The test results show that the *dhajji-dewari* system of buildings possesses tremendous resilience against lateral forces. The function of connections, especially the connections between the vertical posts and bottom plate, control the performance of the system. The test results also indicate that although masonry infill does not contribute to lateral load capacity, it significantly increases the energy dissipation capacity of system. The data accrued from the tests has been used in nonlinear static push-over analysis of the numerical models to develop simplified analytical tools for facilitating lateral load performance evaluation of *dhajji* structures. [DOI: 10.1193/1.4000051]

INTRODUCTION

Dhajji-dewari is the name given to a traditional timber-braced frame with random rubble masonry infill construction practiced mainly in Kashmir, but also found in some mountainous northern parts of Pakistan and India (Figure 1). *Dhajji* means "interconnected" or "patchwork quilt" and *dewari* means "wall" in the local Kashmiri language, therefore *dhajji-dewari* means an interconnected, or patchwork-quilt, wall. As the wall is interconnected by bracers and contains the masonry patchwork used as infill within the timber framework, the name fits the system very well. *Dhajji* buildings are mostly single-story structures with wooden pitched roofs, but two-story structures also exist in some locations.

Similar types of buildings are also found in other parts of the world. In Britain, they are called *half-timbered* (because the frame is timber and the infill is masonry); in Germany, *fachwerk* (framework); and in France, *colombage* ("half-timber" in French; Langenbach 1989, Gülkan and Langenbach 2004). In the cities of Safranbolu and Istanbul, Turkey, *baghdadi, himis,* and *dizeme* are traditional timber-frame systems, differentiated mainly in the choice of infill (Gülkan and Langenbach 2004, Doğangün et al. 2006).

[a] Earthquake Engineering Center Department of Civil Engineering, KP UET Peshawar, Pakistan
[b] Technical Advisor, Swiss Agency for Development and Cooperation

Earthquake Spectra, Volume 28, No. 3, pages 835–858, August 2012; © 2012, Earthquake Engineering Research Institute

Figure 1. A typical *dhajji* house.

The seismic performance of these traditional timber-braced frame systems in almost all the aforementioned cases has been found to be exceptionally resilient to earthquake shaking (Spence and Coburn 1984, Gülhan and Güney 2000, Tobriner 2000, Cardoso et al. 2003, 2004). The closely spaced vertical posts, horizontal and diagonal bracing, and the inherent property of wood to be flexible without breaking when bent back and forth during an earthquake contribute to the outstanding performance of this system.

The performance of *dhajji-dewari* in the 2005 Kashmir earthquake is yet another proof of the consistently earthquake-resilient behavior of this system (Rai and Murty 2005, Mumtaz et al. 2008, Schacher and Ali 2008). Keeping in view the good performance of *dhajji*, the Earthquake Reconstruction and Rehabilitation Authority (ERRA), the official body of the government of Pakistan responsible for reconstruction and rehabilitation in the earthquake-affected areas of Pakistan and Pakistan-administered Kashmir, encouraged its use for construction of housing units in the far-flung mountainous earthquake-hit areas where the system was already known but had fully or partially disappeared over the years.

The relevant literature survey indicates that various research studies on the seismic response of timber-braced frames have been conducted. Quasistatic tests on typical *goaila* walls (Cóias and Silva 2002) and Italian traditional timber-framed walls (Ceccotti et al. 2006) have shown that the walls in each case were able to dissipate energy over many cycles without losing their structural integrity. A more comprehensive study comprising several static and dynamic tests has been conducted on a variety of connections using different diameter bolts and high-strength glulam rivets with steel side plates (Popovski et al. 1998a, 1998b, 1999, 2002; Popovski and Karacabeyli 2006, 2008). Results from quasistatic tests on riveted connections, diagonal bracers, and moment-resisting portal frames by these researchers have

shown that timber rivets are suitable for such wood-based structural systems in earthquake-prone areas.

The research presented in this paper comprises experimental and numerical investigations conducted on typical *dhajji* walls constructed in the field in order to quantify the seismic capacity of *dhajji* structures. The experimental work included in-plane, quasistatic lateral cyclic load tests on three full-scale walls to investigate their in-plane lateral strength, stiffness, ductility, energy dissipation, and damage mechanism. Additionally, tension and bend tests on individual connections were also conducted for their further use in numerical modeling. The numerical study included static pushover analysis for different case-study walls in order to develop a simplified analytical model to evaluate the strength of *dhajji* walls. Additionally, elastic dynamic analysis (EDA) and incremental dynamic analysis (IDA) were carried out on simplified shear-type, multi-degree-of-freedom (MDOF) mathematical models to evaluate the response modification factor (R) for *dhajji* buildings.

EXPERIMENTAL PROGRAM

DETAILS OF TEST SPECIMENS

Three *dhajji* walls (DW-1, DW-2, and DW-3) were constructed in the EEC laboratory from three sets of members having cross-sectional dimensions 100 mm × 100 mm, 50 mm × 100 mm, and 25 mm × 100 mm, as shown in Figure 2. These are the most common sizes used in the field. The 100 mm × 100 mm members were used as main posts and main horizontal bands. The 50 mm × 100 mm members were used as studs and timber pieces of secondary horizontal bands. The 25 mm × 100 mm members were used as cross bracers. The length of

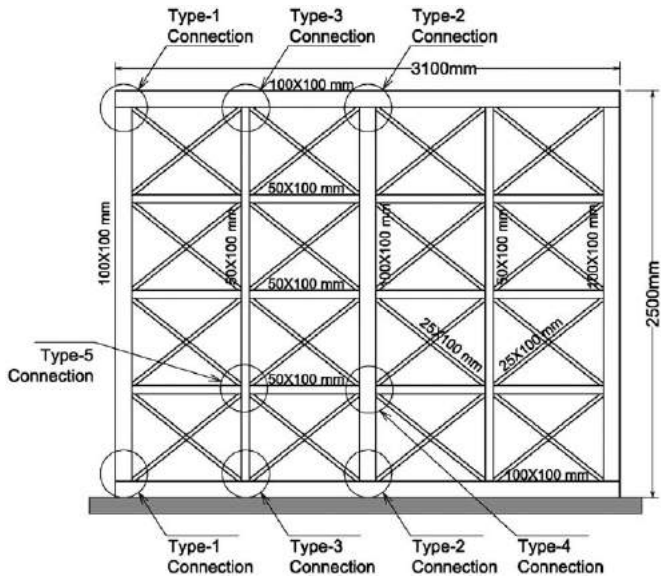

Figure 2. Details of member sizes and types of connections used in *dhajji* wall specimens.

Table 1. Mechanical properties of timber used in the construction of the walls

Timber sample #	Compressive strength parallel to grain (MPa)	Tensile strength perpendicular to grains (MPa)	Modulus of rupture (MPa)	Modulus of elasticity (MPa)
1	23.54	2.35	65.90	4439.67
2	27.85	1.57	70.22	2988.18
3	27.07	1.57	66.19	3441.55
4	28.93	2.35	62.57	3296.02
Average	**26.87**	**1.96**	**66.19**	**3345.24**

the test specimens was kept equal to 3,100 mm, and the height was kept to 2,500 mm, equal to a typical story height. A vertical dead load of 2.0 kN was applied through sand bags placed on top of each main post to simulate the load from a roof truss. Table 1 gives the mechanical properties of the timber used in the construction of wall specimens tested according to the British Standard Methods of Testing Small Specimen of Timber (BS 373:1957).

Wooden nails made of mild steel having a yield strength of 250 MPa were used to fix the connections. The details of various connections, Types 1 to 5, used in the construction of these walls are given in Figure 3. The main vertical posts and studs were connected to the top and bottom plate through Types 1 to 3 tennon and mortise connections using 75 mm long, 4.5 mm round nails. The intermediate horizontal wooden pieces were connected to the main posts and to the studs through Types 4 and 5 connections, respectively. Each cross bracer was connected to the vertical post using two 50 mm long, 3.5 mm round wooden nails. Various stages of the walls' construction are shown in Figure 4.

In the construction of all three specimens, the wooden frames used were identical. In DW-1, the infill comprised a stone-to-mud ratio of 9:1 (hard infill), whereas in DW-2, the ratio was 7:3 (soft infill), to represent the most common practice in the field. Sieve analysis of stones used in the infill indicated that 95% of the stones were 37.5 mm to 75 mm size. The remaining 5% consisted of 12 mm to 25 mm small stone fragments. Similarly, the size distribution of clay showed that 20% of the material consisted of 1.8 mm, 20% of 2.36 mm, 20% of 600 mm, and 40% of 300 mm to 150 mm clay particles. It was not possible to conduct any type of stand-alone test on infill due to the very fragile nature of the infill assemblage.

DW-3, the third specimen, was tested without any infill. The purpose of testing DW-3 was to ascertain the effect of infill in the structural behavior of *dhajji* buildings. All three wall specimens were fixed to a 150 mm thick reinforced concrete footing using three 10 mm round mild steel bolts having yield strength of 250 MPa.

It was observed in the tests on walls that the lateral load response of the system was mainly controlled by the connections between vertical posts and bottom plate. Therefore to evaluate the capacity of these connections independently, bending and tension tests were performed on 18 samples of Type 1, 2, and 3 connections. The sizes of the members in the connection samples were kept equal to that used in the walls. The height of the each sample was kept 30 cm.

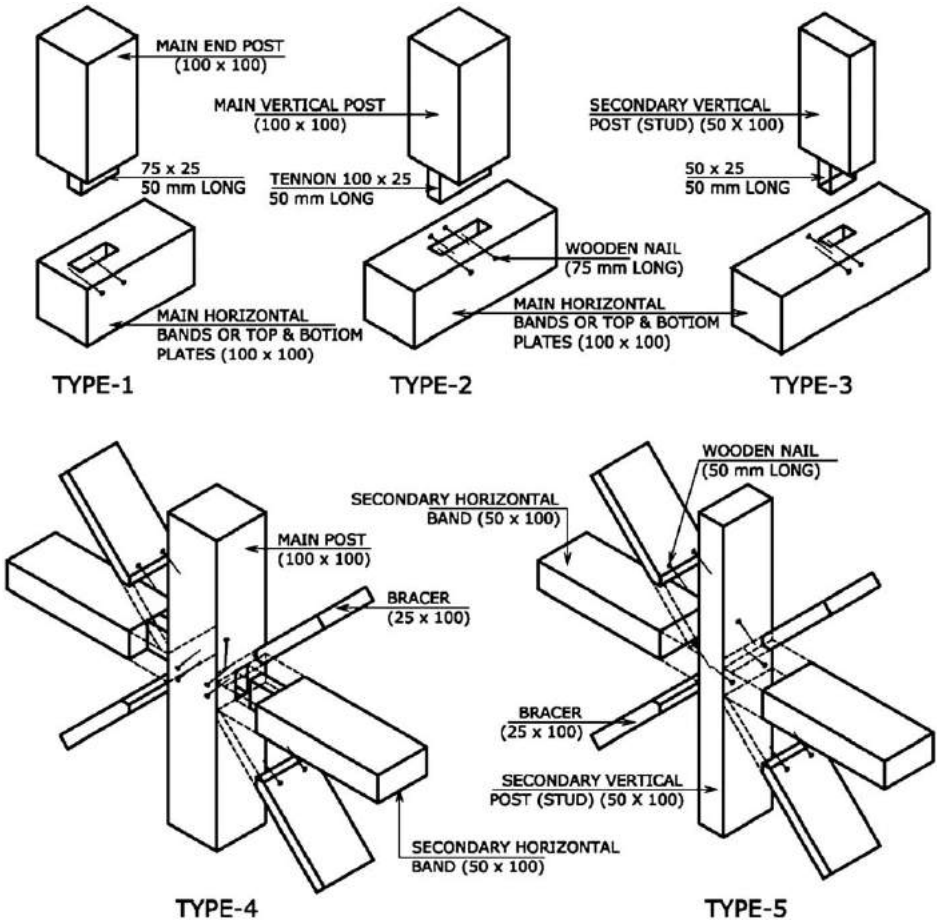

Figure 3. Details of various connections used in *dhajji* wall specimens.

TEST SETUP AND PROCEDURE

The experimental test setup for wall tests is shown in Figure 5. The reinforced concrete footing was fixed with the strong floor of the laboratory. Horizontal load was applied through a hydraulic jack attached to the top horizontal wooden member of the wall. Horizontal load was measured through a 500 kN capacity load cell. Hinges were provided at both the ends of hydraulic jack to release the horizontal and vertical rotations. Eight displacement transducers numbered from 1 to 8 were used to measure displacement. All the gauges were connected to a data acquisition system. Restraints were provided to restrict the out-of-plane movement of the wall but allowing free in-plane movement. In-plane displacement measured with gauge-01 was used as the control displacement.

All walls were subjected to increasing intensities of quasistatic cyclic displacement. Each displacement cycle consisted of loading the specimen to a specified displacement level, unloading to zero displacement, reloading in the negative direction to the same specified

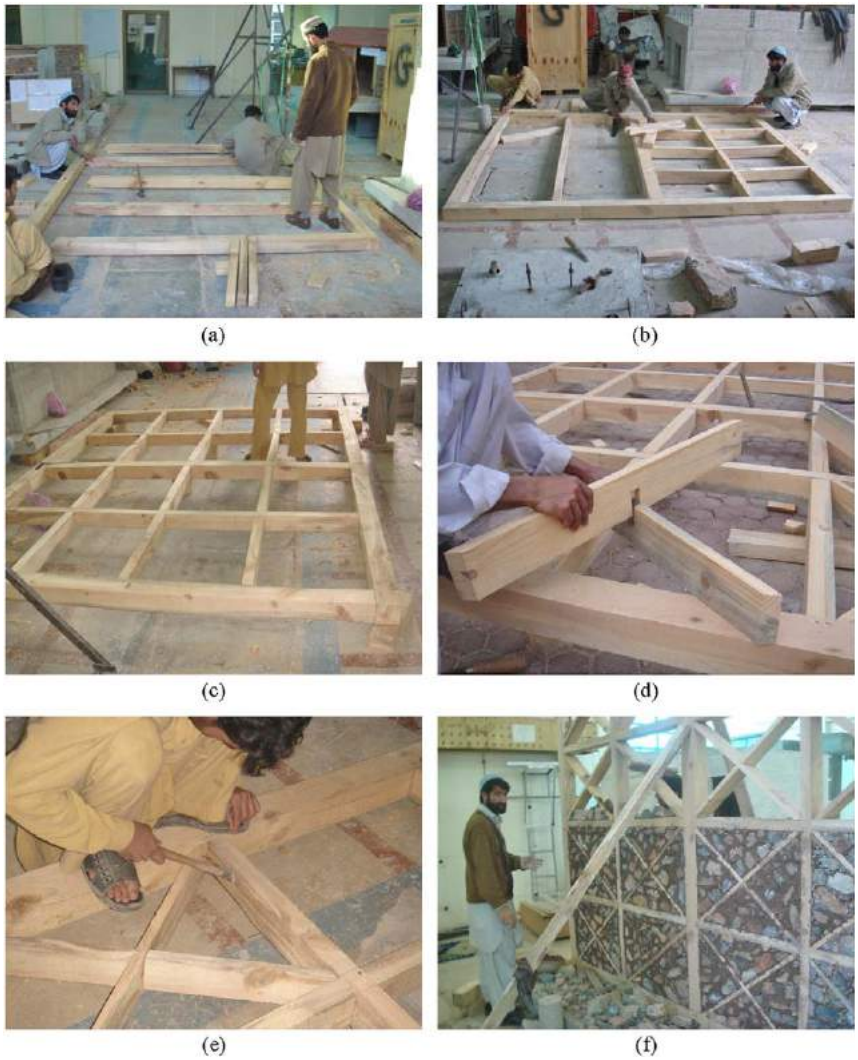

Figure 4. Various stages of *dhajji* walls construction: (a) Main frame of *dhajji* walls, (b) connecting horizontal elements, (c) complete *dhajji* frame without bracers, (d) connection of bracers, (e) nailing of the bracers, and (f) stone filling of the timber panels.

displacement and again unloading to zero displacement. Each displacement cycle was repeated three times.

In the case of DW-1, the test was carried out with displacement increment of 1.0 mm up to 4.0 mm cycles, 2.0 mm increment up to 30 mm cycles, 5.0 mm increment up to 60 mm cycles and 10 mm increment up to the end of the test. Since there was no appreciable load taken by the wall during 1.0 mm displacement cycle, test on DW-2 was started with 2.0 mm displacement cycle. The test was conducted with displacement increments of 2.0 mm up to

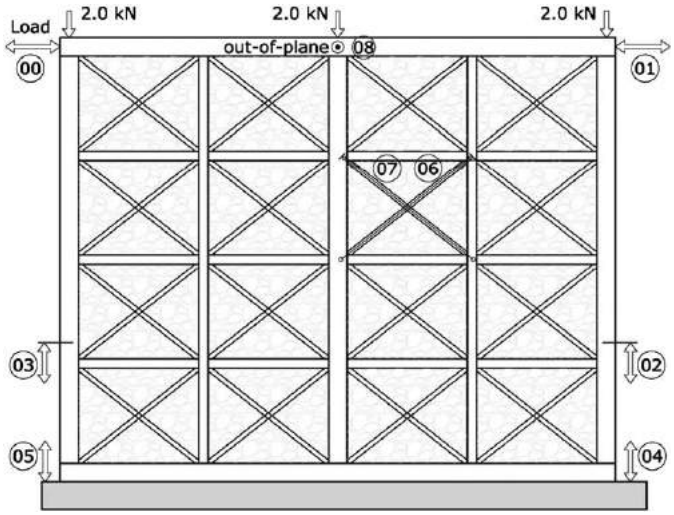

Figure 5. Sketch of experimental test set up.

10 mm cycles, 5.0 mm up to 50 mm cycles and 10 mm up to the end of the test. In the case of DW-3, the test was carried out at displacement increments of 5.0 mm up to 40 mm cycles and 10 mm up to the end of the test.

A total of 18 tests, with three samples each in bending and tension for type 1, 2, and 3, connections were conducted. The test set-up for tests is shown in Figure 6. The base plate of each sample was connected to a rigid platform using round mild steel bolts having yield strength of 250 MPa. All tests were conducted monotonically and data for load deformation curves was obtained using displacement transducers. During the bending test, a transducer was attached laterally at a height of 20 cm from the base of the connection, whereas in the tension test, it was attached vertically along the direction of applied tensile force.

Figure 6. Set up for bending and tension tests on connection specimens: (a) Bending test and (b) tension test.

TEST RESULTS AND DISCUSSION

FORCE-DEFORMATION BEHAVIOR AND DAMAGE MECHANISM OF WALLS

Walls with Infill DW-1 and DW-2

Figures 7 and 8 show lateral load versus drift ratio envelope curves, cyclic response and damping ratio versus drift ratio curve, respectively, for the walls with infill DW-1 and DW-2. Drift ratio is the ratio of top lateral displacement to height of the wall and is expressed as percent drift. During the test on wall DW-1, an unexpected electric power supply failure

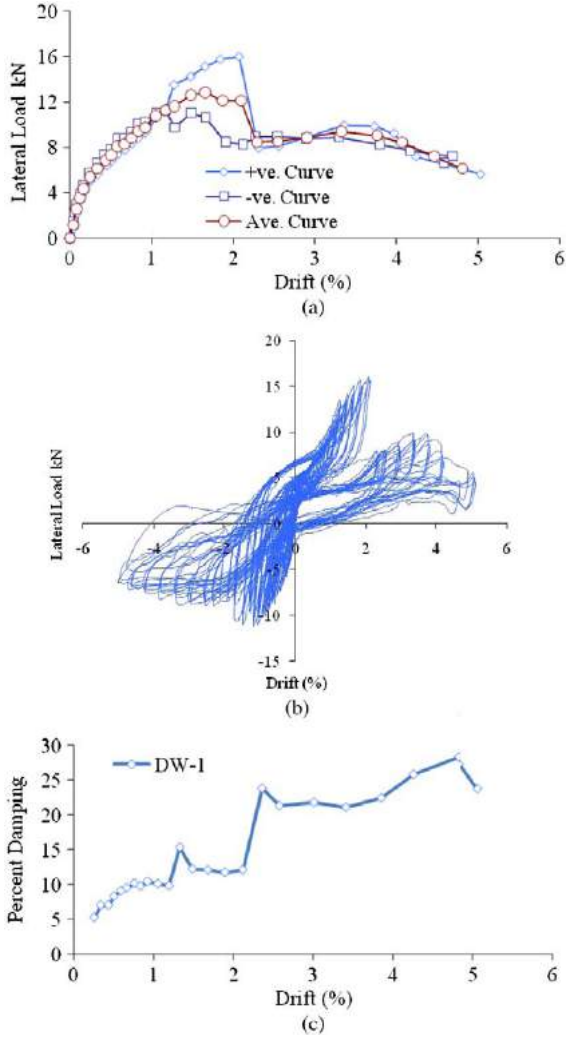

Figure 7. Force deformation parameters for wall DW-1: (a) Lateral load versus drift ratio envelope curves, (b) hysteretic diagram, and (c) damping ratio versus percent drift.

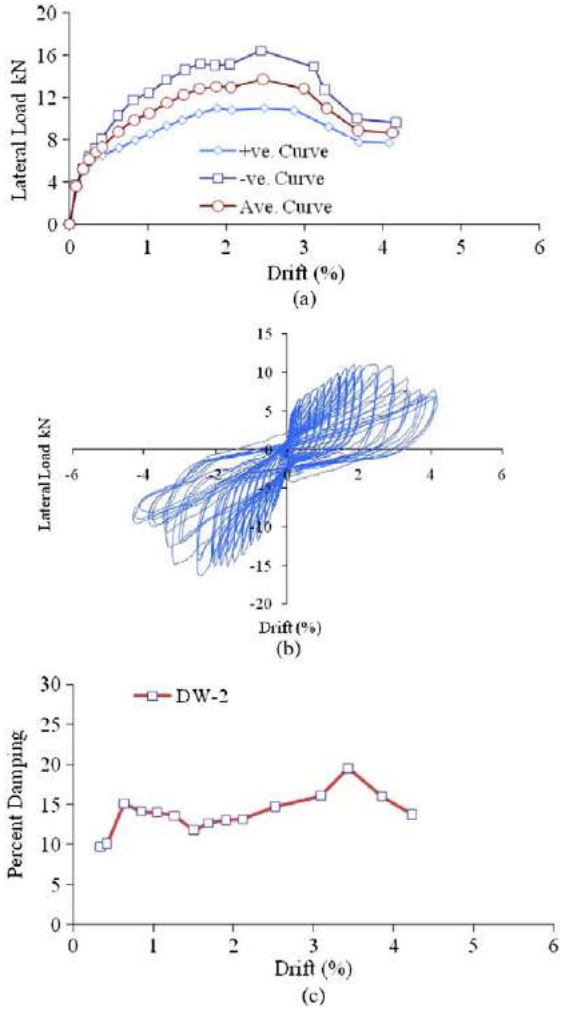

Figure 8. Force deformation parameters for wall DW-2: (a) Lateral load versus drift ratio envelope curves, (b) hysteretic diagram, and (c) damping ratio versus percent drift.

caused about one hour break in the test. The specimen remained loaded during this break, but the deformation values during this hour could not be recorded. The two distinct branches instead of one set of hysteresis loops in Figure 7b reflect this gap clearly.

Figures 7 and 8 show the positive (pushing), negative (pulling), and average lateral load versus drift ratio envelope curves for the walls. Though both positive and negative load curves mostly follow the same profile before the peak value of the lateral load, the difference between the peak values on the curves of the two load cycles can be clearly seen. This difference is an indication of the variability in the capacity of connections mainly due to human factor involved in making the connections along with some uneven role of infill in the

positive and negative load cycles. The post peak response is however again similar in the positive and negative load cycles after failure of the type 1 connections (end vertical post connections) at the bottom of both ends of the wall.

The average envelope curve for both DW-1 and DW-2 shows three steps variation in the slope. The first part of the curve, which is essentially a linear elastic portion and relatively steep, extends up to a drift of 0.15%, corresponding to 35% peak resistance. During this stage, both the walls were deforming in a pure shear mode without showing any signs of rocking, and the infill was fully contributing to the stiffness of the walls. In the second part, from 0.15% to 1.5% drift corresponding to values of 35% to 90% peak load, a gentle decrease in the slope of the curve can be seen, indicating a reduction in the effective stiffness of the walls. In this stage, the walls demonstrated a combination of shear and rocking behavior, with the first visible sign of rocking occurring at around 0.3% drift. The shear distortions were causing opening and closing of bracers and intermediate connections and rocking were causing the pulling of the tennon from the mortise at the bottom of all vertical posts, but more extensively at the main end vertical posts. In the third stage above 1.5% drift, the behavior of the walls was predominantly controlled by rocking occurring at the bottom of the main end posts. However, the sliding of the intermediate horizontal members, bracers, and stone masonry was still taking place and continued until the end of the test. The test ended at the drift limits of 5.0% for DW-1 and 4.20% for DW-2 when the tennon of both the main end posts were completely pulled out from the mortise in the base plate. Damage to the walls DW-1 and DW-2 at various stages throughout the test is shown in Figure 9.

The hysteresis loops in Figures 7 and 8 initially show a soft and then a stiffening effect, with increasing displacement, which indicates that the load is initially consumed in working against the connection tolerances before they are fully mobilized to offer resistance to the increasing lateral load. The flat part of the hysteresis diagram toward the end of the test is an indication of the system instability due to free rocking of the posts about the base plate primarily in the form of pulling of tennon from the mortise. The overall shape of the loops shows that before the system finally fails, it is capable of dissipating substantial amount of energy in numerous load cycles.

The equivalent viscous damping has been calculated from the force-deformation hysteresis loops using the expression given in Equation 1:

$$\xi_{eq} = \frac{E_d}{2\pi E_{inp}} \tag{1}$$

where E_d is the dissipated energy equal to the area of a hysteresis loop and E_{inp} is the input energy equal to the sum of half of the product of maximum load and the corresponding displacement in positive and negative directions. Figures 7 and 8 show that damping increases with drift demand from 5.0% to 25% for DW-1 and 10% to 20% for DW-2, indicating a favorable condition for the system in earthquake shaking.

Walls without Infill DW-3

Figures 10a, b, and c show lateral load versus drift ratio curves, hysteretic diagram, and variation of damping with drift ratio respectively for wall DW-3 having no infill.

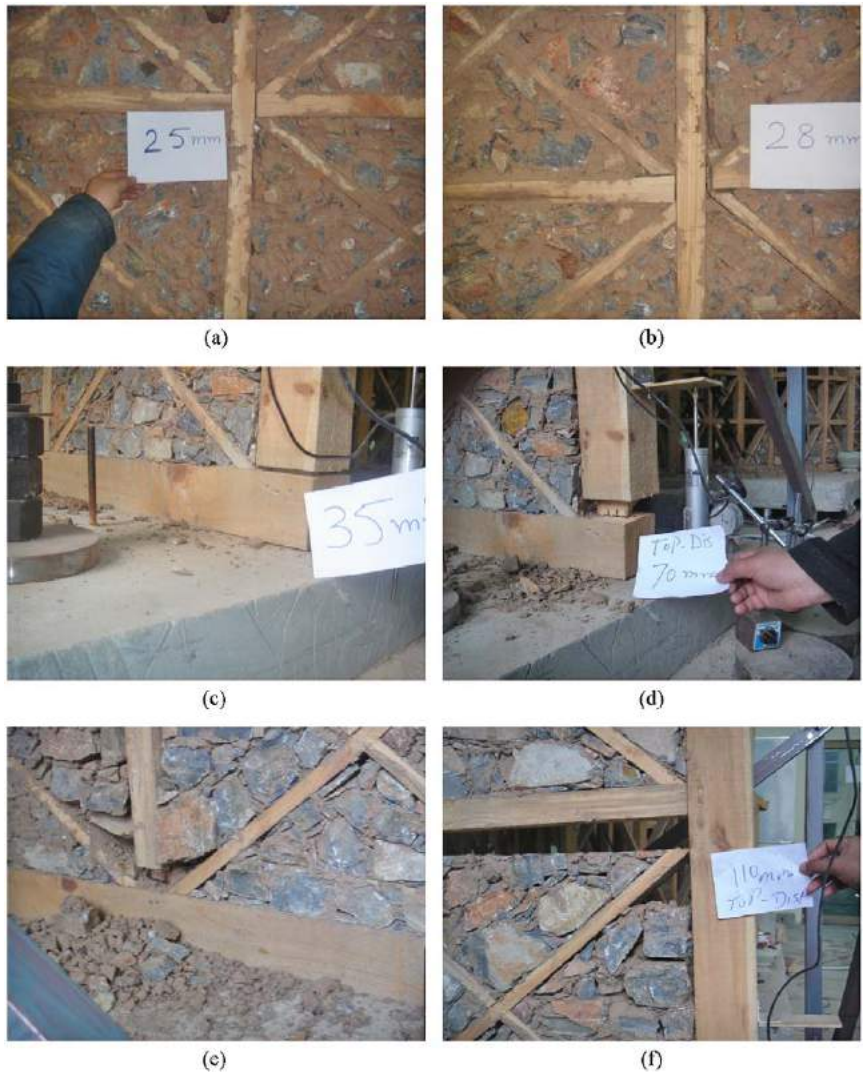

Figure 9. Damage observed in DW-1 and DW-2 during various stages of tests: (a) Falling of Infill at 1% drift, (b) separation of horizontal element at 1.12%, (c) pulling out of tennon at 1.4% drift, (d) complete pulling out of tennon at 2.8% drift, (e) pulling out of secondary vertical post at 4.4% drift, and (f) separation of bracer at 4.4% drift.

Figure 10a shows that the positive and negative load cycle curves follow the same path throughout the load history. The figure also demonstrates that the system enters into the nonlinear range even at the onset of the test, following a gradual decline in the stiffness until the wall attains its peak resistance at a drift of 3.0%. The initial stiff linear elastic part, as is seen in walls DW-1 and DW-2, is absent in wall DW-3 for the obvious reason

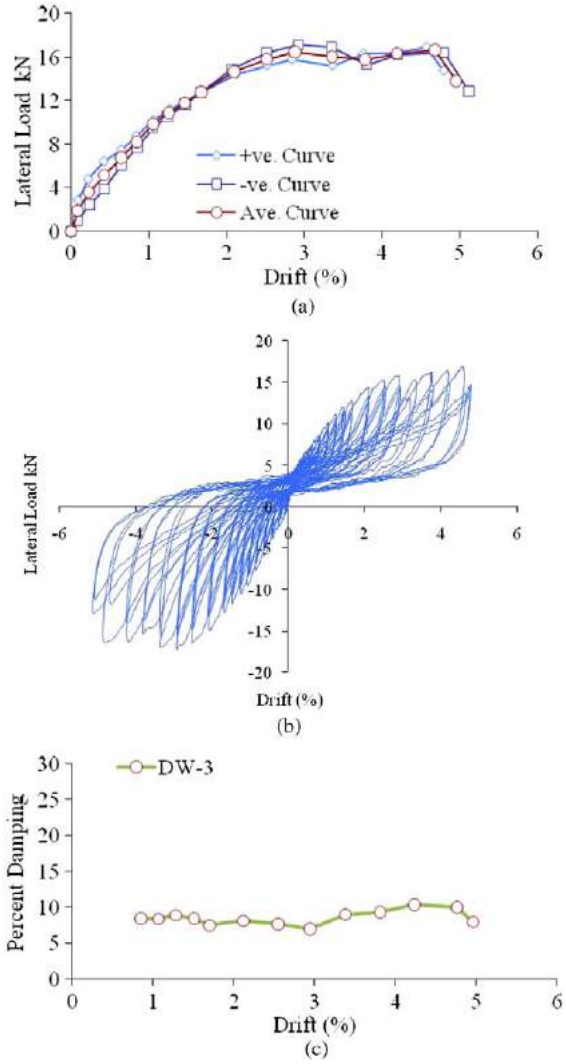

Figure 10. Force deformation parameters for wall DW-3: (a) Lateral load vs drift ratio envelope curves, (b) hysteretic diagram, and (c) damping ratio versus percent drift.

of nonexistence of infill. As there was no interaction of infill with the timber framework, wall DW-3 was much more flexible than walls DW-1 and DW-2. The rocking started at a very early stage, corresponding to a value of 0.1% drift. Though shear distortion of timber panels was causing the opening of the connections, which continued until the end of the test, the rocking behavior in this case was more dominating than that of walls DW-1 and DW-2 at the same drift ratios. The wall finally reached its capacity at larger deformation than that of walls DW-1 and DW-2 but approximately at the same lateral load. Damage to the walls at various stages during the test is shown in Figure 11. The failure in this case also occurred when the

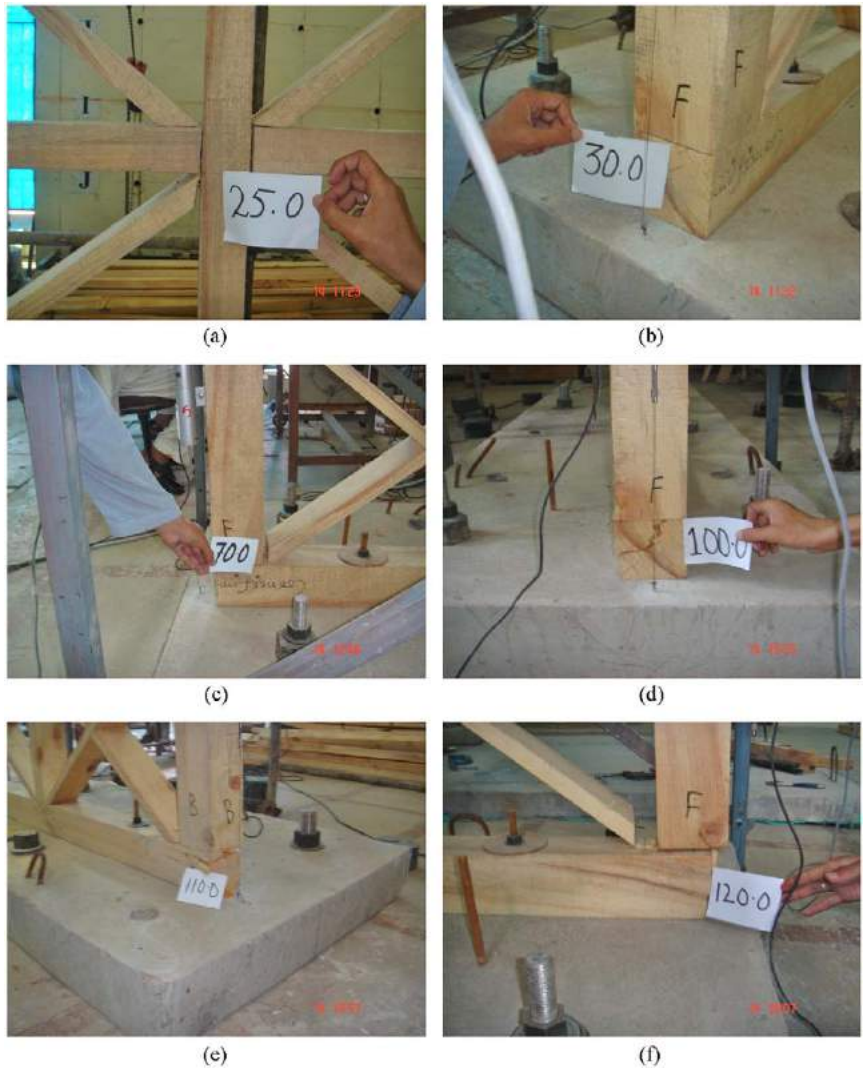

Figure 11. Damage observed in DW-3 during various stages of tests: (a) Opening of bracer at 1% drift, (b) pulling out of tennon at 1.2%, (c) separation of bracer at 2.8% drift, (d) rocking at 4% drift, (e) breakage of dassa at 4.4% drift, (f) separation of bracer at 4.8% drift.

tennon of main end posts were completely pulled out from the mortise of the wall plate. Thus, except for a few load cycles where the infill interacted with timber framework in the walls DW-1 and DW-2, the overall behavior of all the walls was almost similar. The connections between the main vertical posts and wall plate remained the main source of energy dissipation, thereby controlling the overall response of the walls with a very marginal role of the infill in the lateral load capacity of walls.

The hysteretic diagram for wall DW-3 is more symmetric and explicit than those of walls DW-1 and DW-2. Comparatively fewer imperfections due to the careful fixing of connections, as observed during the construction of wall DW-3, and the absence of any role of infill are the two main reasons for this behavior of the wall. The variation of damping with drift ratio shows that damping remains almost constant at around 7.0% throughout the load history of the wall DW-3. A significant increase in damping was seen at higher drifts for walls DW-1 and DW-2.

Comparison of the Behavior of Walls

Figure 12 shows a comparison of the force-deformation behavior of all the three walls in the form of average envelope curves and their bilinear approximation. The bilinear curves are obtained from the force-deformation curves based on the equal energy principle (Magenes and Calvi 1997). The yield strength is taken 90% of the measured peak strength. The ultimate drift is taken as the point where the measured peak strength degrades by 20%. The effective stiffness is taken as the slope of the line joining origin with a point on force-deformation curve corresponding to 75% yield strength. Since there was difference in the envelope curves for negative and positive load cycles, the average envelope curve in each case has been used for the calculation of these parameters.

Figure 13 provides a comparison of various force-deformation parameters such as peak and yield strengths, yield and ultimate drifts, and effective stiffness of the three wall specimens. Figure 14 shows a comparison of damping values for all three walls along with a best-fit simplified analytical model developed to estimate the damping of typical *dhajji* walls with infill corresponding to a given drift ratio. The comparison shows that the masonry infill does not significantly affect these response parameters except viscous damping which is higher for the walls with infill than that of the wall without infill. The analytical model for damping is given in Equation 2.

$$\zeta(\%) = 4 \times Drift\ Ratio\ (\%) + 5.0 \tag{2}$$

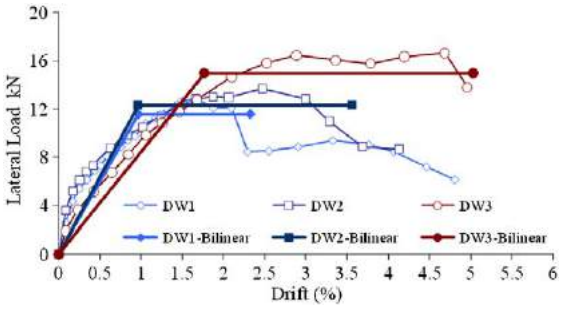

Figure 12. Average envelope curve with bilinear approximation for the three walls.

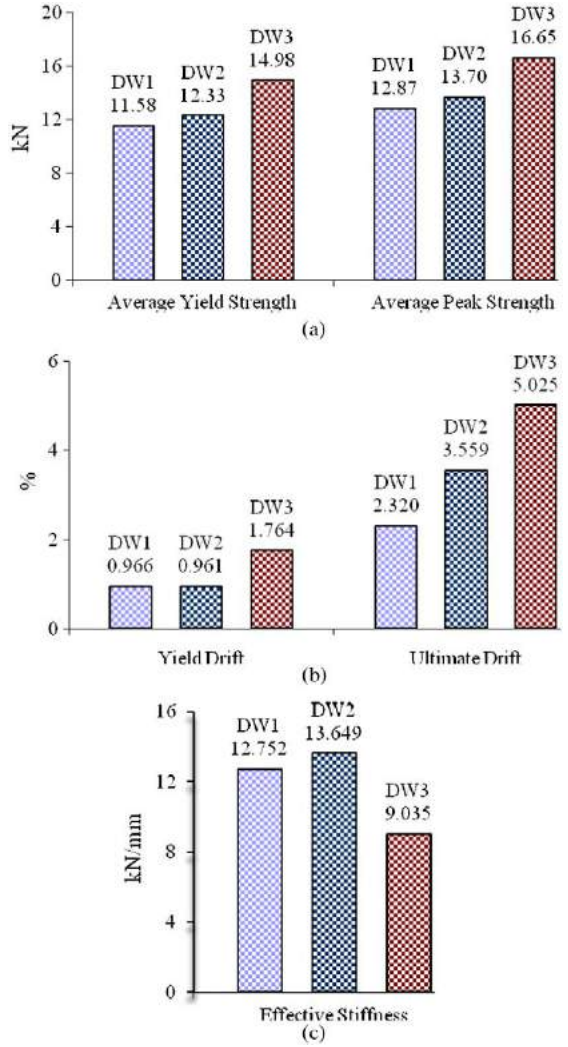

Figure 13. Comparison of various force-deformation parameters of all the three walls: (a) Average peak and yield strengths, (b) ultimate drift, and (c) effective stiffness.

CAPACITY OF CONNECTIONS

The moment versus rotation and load versus displacement curves obtained from bending and tension tests on 18 specimens for types 1, 2, and 3 connections are given in Figure 15. The figure shows that type 2 is the strongest and that type 3 is the weakest of the three connections due to the difference in size and number of nails used in these connections. In the type 1 connection, the failure of edge of mortise due to pushing of tennon in the bending test caused a reduction in its bending capacity as compared to type 2 connection, where the base plate was extended on both sides.

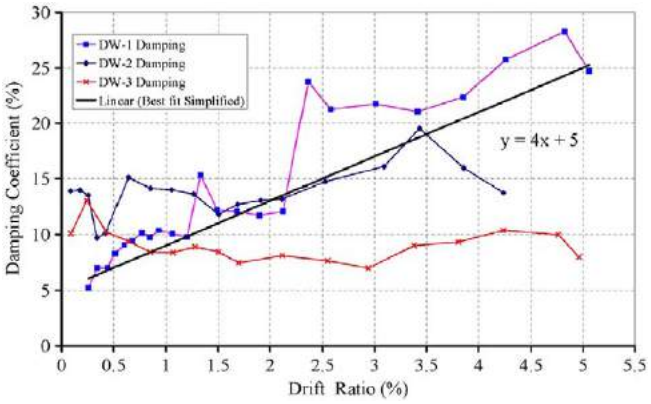

Figure 14. Comparison of damping values for the three walls, along with a best-fit simplified analytical model.

The corresponding idealized average elastoplastic bilinear curves, using the energy balance criteria (Magenes and Calvi 1997), are also shown in the same figure. These elastoplastic curves have been used to idealize the behavior of connections in the numerical model of *dhajji* wall as discussed in the next section.

NUMERICAL INVESTIGATION OF *DHAJJI* WALL STRUCTURES

The finite element–based software SAP2000 v.08 was used for the numerical modeling of the walls. All characteristics of the numerical model were kept similar to the experimental model except infill, which did not exist in the numerical model for the reasons already discussed. The data of respective bending and tension elastoplastic curves were assigned to types 1, 2, and 3 connections in the model, using the "hinge property" function of SAP2000. Moment releases were applied to the ends of cross bracers and interior horizontal members to simulate the free rotation behavior of these connections as observed during the tests on the walls. Moreover as these members did not offer any resistance to tensile forces, the tension limit of these members was set at zero whereas the compression limit was set equal to the compressive strength of member. The model was analyzed using nonlinear static pushover analysis option of the software to obtain capacity curve (pushover curve) of the walls. A snap shot of the numerical model of wall in SAP2000 is shown in Figure 16. The pushover curve along with experimentally obtained curves is given in Figure 17. The figure shows that the pushover curve matches very well with the experimental curves, which indicates that nonlinear static pushover analysis of simplified numerical models ignoring the effect of infill and employing the elastoplastic curves of connections can be very conveniently used for capacity evaluation of *dhajji* structures.

After validation of numerical model against the experimental results, eight numerical wall models from 760 mm to 6,000 mm with a length increment of 760 mm were analyzed to obtain a pushover curve in each case. Subsequently, elastoplastic bilinear curves using the energy balance criteria (Magenes and Calvi 1997) were developed from each pushover

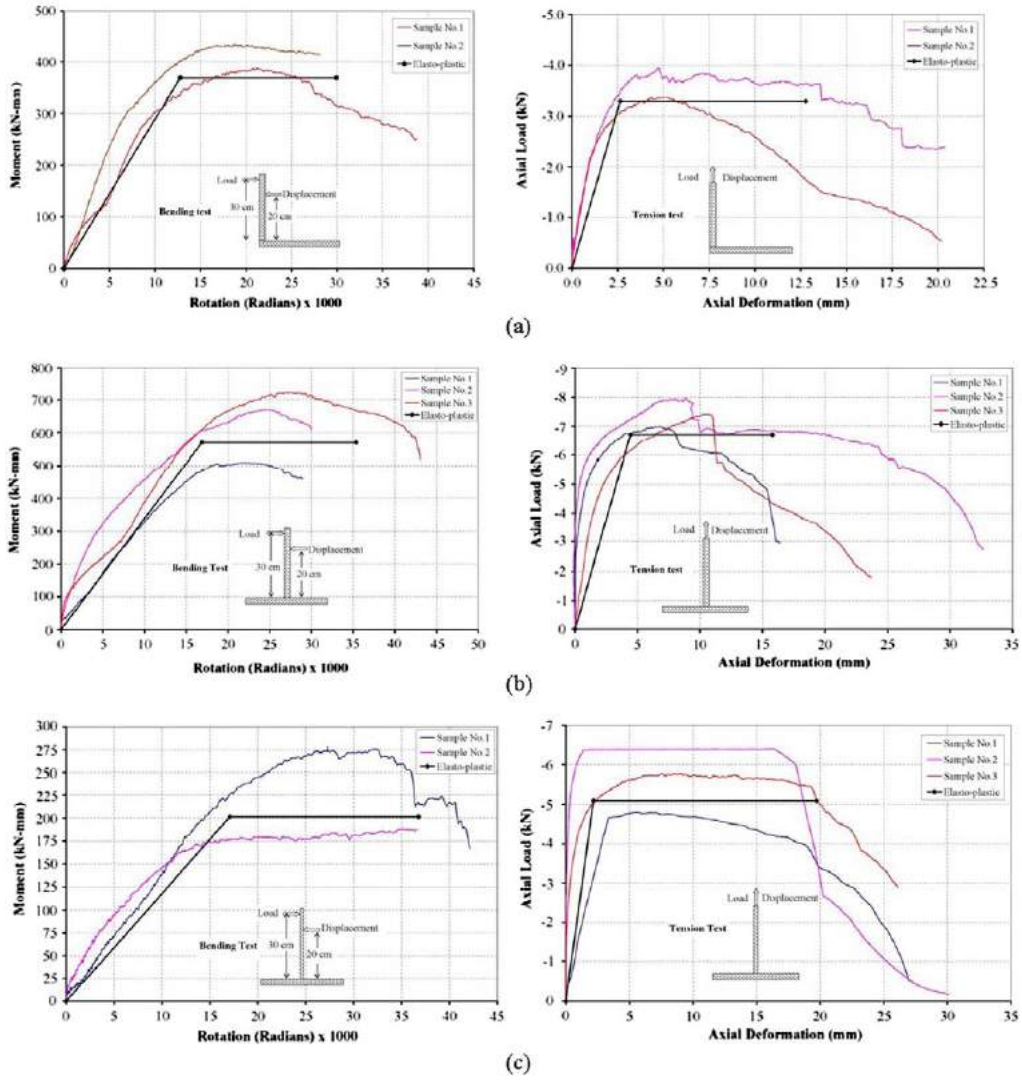

Figure 15. Moment versus rotation, load versus displacement and average elastoplastic curves obtained from bending and tension tests for (a) type 1, (b) type 2, and (c) type 3 connections.

curve to obtain maximum capacity (H), yield displacement (d_y), and ultimate displacement (d_u). The data obtained from each case study was plotted against the respective wall length to derive the following best fit simplified analytical models as given in Equations 3, 4, and 5:

Model for lateral strength, H (kN):

$$H = 2.0 \times L^{1.7} \tag{3}$$

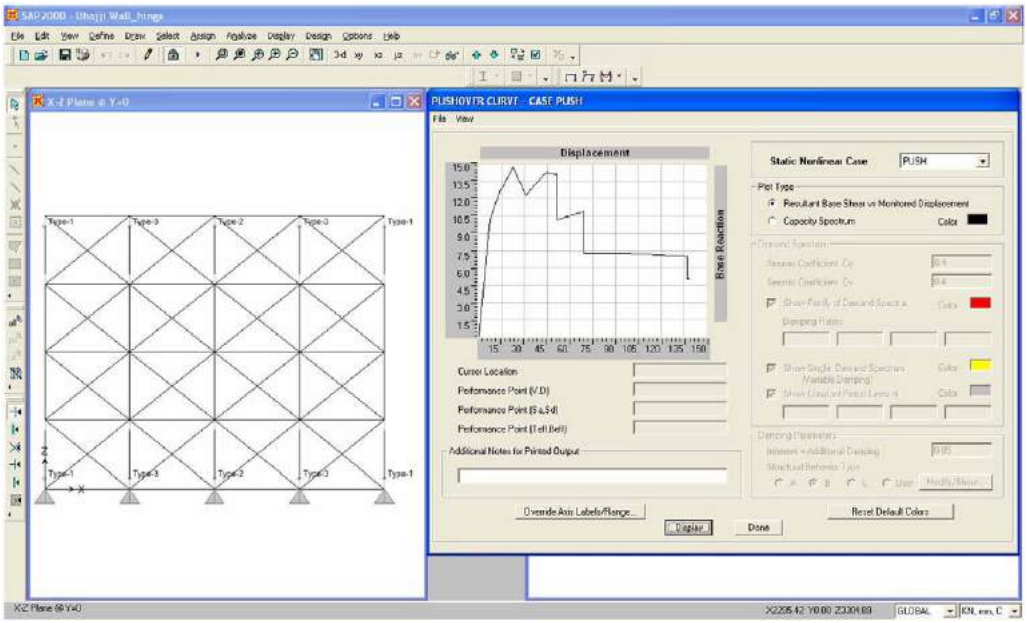

Figure 16. Snapshot of numerical model and pushover curve in SAP2000.

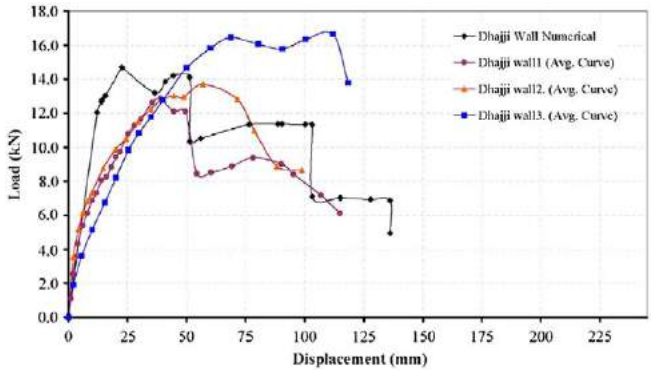

Figure 17. Experimental and numerical capacity curves for *dhajji* walls.

Model for yield displacement, d_y (mm):

$$d_y = 20\,L^{-0.3} \tag{4}$$

Model for ultimate displacement capacity, d_u (mm):

$$d_u = 90\,L^{-0.3} \quad \text{OR} \quad d_u = 4.5\,d_y \tag{5}$$

where L = length of wall in meters.

Using these equations, in-plane capacity curve of a *dhajji* wall can be easily developed. Subsequently, considering the rigid diaphragm behavior, the overall in-plane capacity of a *dhajji* building can be computed from the superposition of capacity curves for all walls along the same direction.

The rigid diaphragm behavior for *dhajji* construction is an assumption. In reality, it would depend on the actual rigidity of the roof, which may vary from place to place. Given the condition that a pitched wooden truss roof well-anchored to the timber frame and having a horizontal cross bracing in plan is the typical roofing system used for *dhajji* construction and that length of such roofs is relatively small (normally 4 m to 5 m), it is believed that they are fairly rigid in plan to behave very closely as a rigid diaphragm.

RESPONSE MODIFICATION FACTOR *R*

Three different techniques have been used to compute R for *dhajji* structures in order to take care of the inherent uncertainties in the definition of R. The first approach is based on the equal energy principle using the classical analytical model:

$$R = \sqrt{2\mu - 1}, \quad \mu = \frac{d_u}{d_y} \tag{6}$$

where μ represents the displacement ductility, d_u represents the ultimate displacement capacity, and d_y represents the yield displacement. The energy-balance criterion is used due to the fact that the fundamental vibration period of tested walls (0.28 for DW-1; 0.24 for DW-2; 0.17 seconds for DW-3) lies on the constant acceleration part of the design spectra of Building Code of Pakistan, Seismic Provision (BCP-SP2007). The same approach, but with different spectra has been used by other researchers (Tomazevic and Weiss 2010).

In the second method, R is computed as given in Equation 7:

$$R = \frac{F_e}{F_d} \tag{7}$$

F_e represents the force demand on the idealized elastic structure having 5% viscous damping, and F_d represents the minimum required design strength, which can be computed for different structural system of *dhajji* walls using the experimental strength models.

The third approach, given in Equation 8, is based on the incremental dynamic analysis (IDA) of an inelastic structure following the Kappos model (Kappos 1991).

$$R = \frac{PGA_{ultimate}}{PGA_{yield}} \tag{8}$$

$PGA_{ultimate}$ represents the target peak ground acceleration (PGA) of ground motions causing the collapse of structure and PGA_{yield} represents the target PGA causing the yielding of structure.

A simplified multi-degree-of-freedom (MDOF) shear-type model with elastic frame elements, having either linear or nonlinear lumped inelasticity hinges, was developed for *dhajji* structures using equivalent frame idealization of walls for linear and nonlinear dynamic time

history analyses (see Figure 18). The dashed lines show the portion of wall mass (masonry and wood) lumped at multiple levels. The additional mass from the floor is considered at the top level. The nonlinear hinge was assigned to the model only at the bottom frame element, as the nonlinearity in the tested walls was observed mainly at the bottom.

For both linear and nonlinear dynamic analysis, ten natural accelerograms compatible with design spectra of BCP-SP 2007 were selected. For elastic dynamic analysis (EDA), all accelerograms were scaled to a PGA of 0.6 g, while for IDA, the accelerograms were scaled to different level of PGA in order to reach the ductility capacity of wall. Figure 19 shows the comparison between experimental and simplified numerical cyclic response as well as nonlinear response of a *dhajji* wall to target PGA of 0.6 g for Northridge 1994–Canoga Park-Topanga Can. In the case of IDA, a demand chart was also developed between PGA and ductility demand, which was then interpolated to compute PGA at yielding and

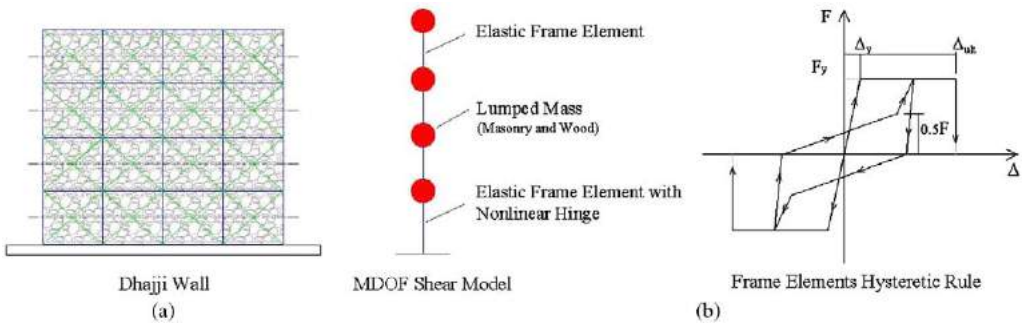

Figure 18. (a) Mathematical model of *dhajji* wall system and (b) nonlinear force-displacement hysteretic response of frame elements.

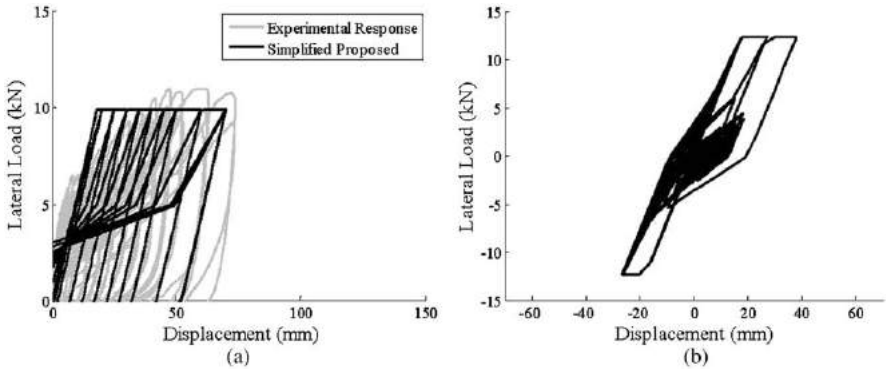

Figure 19. Comparison between (a) experimental and simplified numerical cyclic response and (b) nonlinear response of a *dhajji* wall to target PGA of 0.6g for Northridge 1994–Canoga Park-Topanga Can.

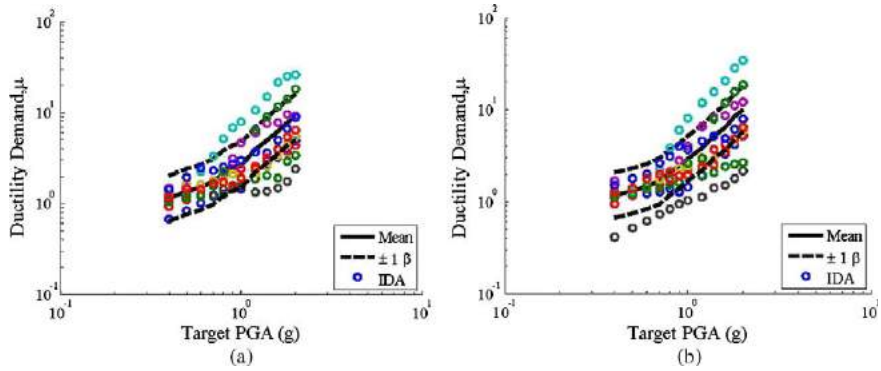

Figure 20. Ductility demand on *dhajji* structures through IDA: (a) DW-1 and (b) DW-2.

Table 2. Response modification factor for *dhajji* wall structures

		R					
Wall	Ductility	Equal Energy	IDA	EDA	Mean	Recommended	Remarks
DW-1	2.52	2.01	1.85	1.47	1.78	2.00	The values correspond to the characteristic estimate of *R* for IDA and EDA.
DW-2	4.78	2.93	2.49	1.40	2.27		
DW-3	3.00	2.24	–	–	–		

ultimate limit states of the walls, Figure 20. The characteristics demand chart, that is, the 16th percentile value which has 84% chances of exceedance, is used to compute *R*. This approach has been used also by researchers such as Zafar and Andrawes (2011) among others.

The values of *R* resulting from all three approaches are given in Table 2, which shows that an average estimate of 2.0 may be used as an appropriate value for the *R* factor of *dhajji* structures.

CONCLUSIONS AND RECOMMENDATIONS

The following conclusions are drawn from this study:

- The test results show that *dhajji* walls went through numerous load cycles before they started losing their structural integrity at drift ratios of around 1.5%, thus confirming that the *dhajji-dewari* system of buildings possesses tremendous resilience against lateral forces.
- The overall behavior of *dhajji* walls indicates that lateral load capacity of such buildings depends mainly on the performance of timber framework, with no contribution from the infill. The functioning of connections, especially those between the vertical posts and bottom plate, govern the capacity of the system.

- The ultimate strength and ductility of *dhajji* walls are least affected by change in the choice of infill types commonly practiced in the field.
- The damping ratio of walls with infill in the inelastic range increases from 5% to 25% for wall with hard infill and 7% to 20% for wall with soft infill. The damping of wall without infill remains constant at 7% throughout the loading history. Analytical model for typical *dhajji* walls with infill is given as $\zeta\,(\%) = 4 \times Drift\,Ratio\,(\%) + 5.0$.
- The numerical investigation indicates that nonlinear static pushover analysis of simplified numerical models ignoring the effect of infill and employing the elastoplastic curves of connections can be very conveniently used for capacity evaluation of *dhajji* structures.
- Response modification factor R equal to 2.0 can be adopted for *dhajji* buildings under the given conditions.
- The following analytical model is proposed for the capacity evaluation of *dhajji* walls:
  Model for Lateral Strength, $H\ (\mathrm{kN}) = 2.0 \times L^{1.7}$
  Model for Yield Displacement, $d_y\ (\mathrm{mm}) = 20\,L^{-0.3}$
  Model for Ultimate Displacement Capacity, $d_u\ (\mathrm{mm}) = 90\,L^{-0.3} = 4.5\,d_y$
  L = Length of wall in meters
- As the main timber elements did not suffer any damage in all tests, the type of timber used in such system of construction will not affect the overall performance of a structure, provided timber has been properly seasoned and treated against termite attack.
- As walls with X bracing were investigated in this study, the results may not be directly applicable for walls with other types of bracing.

ACKNOWLEDGEMENT

The authors greatly acknowledge financial support from the Board of Advanced Studies and Research at Khyber Pakhthunkhwa University of Engineering & Technology Peshawar (KP UET Peshawar) Pakistan, Higher Education Commission Islamabad, Rectors' Conference of the Swiss Universities of Applied Sciences (KFH), and Philip Morris International. The authors acknowledge the support of Engr. M. Fahim and the lab staff of the EEC, Earthquake Engineering Center at KP UET Peshawar. The authors also acknowledge the support of Maggie Stephenson of UNHABITAT for her valuable suggestions.

REFERENCES

Building Code of Pakistan (BCP), 2007. Seismic provisions, in *Building Code of Pakistan*, Ministry of Housing and Works, Islamabad, Pakistan.

British Standards Institution (BS 373), 1957. *BS 373:1957 Methods of Testing Small Clear Specimens of Timber*, BSI, London.

Cardoso, R., Lopes, M., Bento, R., and D'Ayala, D., 2003. *Historic, Braced Frame Timber Buildings with Masonry Infill ("Pombalino" Buildings)*, Report No. 92, *World Housing Encyclopedia*, Earthquake Engineering Research Institute, Oakland, CA.

Cardoso, R., Lopes, M., and Bento, R., 2004. Earthquake resistant structures of Portuguese old "Pombalino" buildings, *13th World Conference on Earthquake Engineering (13WCEE)*, Vancouver, BC, Canada.

Ceccotti, A., Faccio, P., Nart, M., Sandhaasl, C., and Simeone, P., 2006. Seismic behaviour of historic timber-frame buildings in the Italian Dolomites, *International Wood Committee 15th International Symposium*, Istanbul and Rize, Turkey.

Cóias e Silva, V., 2002. Using advanced composites to retrofit Lisbon's old "seismic resistant" timber framed buildings, *European Timber Buildings as an Expression of Technological and Technical Cultures*, Editions Scientifiques et Médicales, Elsevier SAS, 109–124.

Doğangün, A., Tuluk, Ö., Livaoğlu, R., and Acar, R., 2006. Traditional wooden buildings and their damages during earthquakes in Turkey, *Engineering Failure Analysis* **13**, 981–996.

Gülhan, D., and Güney, İ. Ö., 2000. The behavior of traditional building systems against earthquake and its comparison to reinforced concrete frame systems: experiences of Marmara earthquake damage assessment studies in Kocaeli and Sakarya, *Proceedings of Earthquake-Safe: Lessons to be Learned from Traditional Construction*, Istanbul, Turkey, available at http://www.icomos.org/iiwc/seismic/Gulhan.pdf.

Gülkan, P., and Langenbach, R., 2004. The earthquake resistance of traditional timber and masonry dwellings in Turkey, *13th World Conference on Earthquake Engineering*, Vancouver, BC, Canada, Paper No. 2297.

Kappos, A. J., 1991. Analytical prediction of the collapse earthquake for R/C buildings: Suggested methodology, *Earthquake Engineering and Structural Dynamics* **20**, 167–176.

Langenbach, R., 1989. Bricks, mortar, and earthquakes, *APT Bulletin* **21**, 30–43.

Magenes, G., and Calvi, M., 1997. In-plane seismic response of brick masonry walls, *Earthquake Engineering and Structural Dynamics* **26**, 1091–1112.

Mumtaz, H., Habib Mughal, S., Stephenson, M., and Bothara, J. K., 2008. The challenges of reconstruction after the October 2005 Kashmir earthquake, *NZSEE Annual Conference*, New Zealand.

Popovski, M., Prion, H. G. L., and Karacabeyli, E., 1998a. Seismic behavior of braced timber frames, *Sixth U.S. National Conference on Earthquake Engineering: Seismic Design and Mitigation for the Third Millennium*, Seattle, WA.

Popovski, M., Prion, H. G. L., and Karacabeyli, E., 1998b. Influence of connection details on seismic performance of braced timber frames, *Eleventh European Conference on Earthquake Engineering*, Paris, France.

Popovski, M., Karacabeyli, E., and Prion, H. G. L., 1999. Dynamic response of braced timber frames, *Eighth Canadian Conference on Earthquake Engineering*; Vancouver, BC, Canada.

Popovski, M., Prion, H. G. L., and Karacabeyli, E., 2002. Seismic performance of connections in heavy timber construction, *Canadian Journal of Civil Engineering* **29**, 389–399.

Popovski, M., and Karacabeyli, E., 2006. Seismic behavior of structural systems with riveted connections in timber construction, *8th U.S. National Conference on Earthquake Engineering (8NCEE)*, San Francisco, CA.

Popovski, M., and Karacabeyli, E., 2008. Force modification factors and capacity design procedures for braced timber frames, *14th World Conference on Earthquake Engineering (14WCEE);* Beijing, China.

Rai, D. C., and Murty, C. V. R., 2005. *Preliminary Report on the 2005 North Kashmir Earthquake of October 8, 2005*, Indian Institute of Technology Kanpur, India.

Schacher, T., and Ali, Q., 2008. Timber reinforced stone masonry in northern Pakistan in the context of the post earthquake reconstruction efforts, *International Seminar on Seismic Risk and Rehab of Stone Masonry Housing*, Azores, Portugal.

Spence, R. J. S., and Coburn, A. W., 1984. Traditional housing in seismic areas, *Proceedings of the International Conference at Quaid-i-Azam University*, Islamabad, Pakistan, Miller-K-J, Ed., Cambridge University Press, Cambridge.

Tobriner, S., Wooden Architecture and Earthquakes in Turkey, 2000, *A Reconnaissance Report and Commentary on the performance of wooden structures in the Turkish earthquakes of 17 August and 12 November 1999, Report for the United Nations Centre for Regional Development, Disaster Management Planning*, Hyogo Office, Japan.

Tomazevic and Weiss, 2010. Displacement capacity of masonry buildings as a basis for the assessment of behavior factor: an experimental study, *Bulletin of Earthquake Engineering* **8**, 1267–1294.

Zafar, A., and Andrawes, B., 2011. Response modification factor for reinforced concrete buildings in Pakistan, *Proceedings of the International Conference on Earthquake Engineering and Seismology*, Islamabad, Pakistan.

(Received 11 July 2010; accepted 8 July 2011)